Shannon wavelet transform for solving fractional differential-algebraic equations numerically

Mesut Karabacak, Muhammed Yiğider

Abstract— **In this paper, the numerical solution of fractional differential-algebraic equations (FDAEs) is considered by Shannon wavelets. We derive the wavelet operational matrix of the fractional order integration and by using it to solve the fractional differential-algebraic equations. Two illustrative examples are presented to demonstrate the applicability and validity of the wavelet base technique. To highlight the convergence, the numerical examples are solved for different values of order. The results obtained are in good-agreement with the exact solutions. It is shown that the technique used here is effective and easy to apply.**

Index Terms— **differential-algebraic equations (DAEs), fractional differential-algebraic equations (FDAEs), Shannon wavelets, operational matrix.**

I. INTRODUCTION

Fractional modeling and fractional differential equations has been used widely to deal with some engineering problems in recent years. The main advantage of fractional derivatives lies in that it is more suitable for describing memory and hereditary properties of various materials and process in comparison with classical integer-order derivative. Besides, differential-algebraic equations (DAEs) have been successfully used to characterize for many physical and engineering topics such as polymer physics, fluid flow, electromagnetic theory, dynamics of earthquakes, rheology, viscoelastic materials, viscous damping and seismic analysis. Also differential-algebraic equations with fractional order, which often arise in integrated circuits with new memory materials, have been made in some mathematical models in recent times. As known, fractional differential-algebraic equations usually do not have exact solutions. Therefore, approximations and numerical techniques should be used for them and also the solution of these equations has been an attractive subject for many researchers.
[1-12]

Also, wavelet analysis is a relatively new area in mathematical researches. Wavelets are localized functions which are a useful tool in many different applications: signal analysis, vibration analysis, data compression, solving PDEs, solid mechanics and operator analysis. In many times, wavelets have been used only as any other kind of orthogonal functions, without taking into consideration their fundamental properties. [13,14]

In this paper, we show to use Shannon wavelet bases to solve the fractional order differential-algebraic equations.

This work was supported by Scientific Research Projects (BAP) commission of the Erzurum Technical University. Project Number: 2015/2

Mesut Karabacak, Department of Actuarial Sciences, Faculty of Science, Atatürk University, Erzurum 25240, Turkey (* Corresponding Author)

Muhammed Yiğider, Department of Mathematics, Faculty of Science, Erzurum Technical University, Erzurum /Turkey

Firstly, we derive Shannon wavelet operational matrix of the fractional order integration and then we use the Shannon wavelet operational matrix to transform the fractional order systems into algebraic systems of equations completely.
Finally, we solve this transformed complicated algebraic equations system by Mathematica software.

The paper is organized as follows. In Section 2, we introduce some preliminaries of the fractional calculus theory. In Section 3, some relevant properties of the Shannon wavelet bases and function approximation by these bases are presented. Also, operational matrix of integration for Shannon wavelet is obtained. In Section 4, we demonstrate some numerical examples and we end with some conclusions and remarks in Section 5.

II. PRELIMINARIES AND BASIC DEFINITIONS

A fractional differential-algebraic equation (FDAE) with the initial conditions is defined as the form below [15]

$$\begin{aligned} &D^{\alpha_i}x_i(t) = f_i\left(t, x_1, x_2, \dots x_n, x_1', x_2', \dots x_n'\right) \\ &i = 1,2,3, \dots n-1, \quad t \geq 0 \ ,0 < \alpha_i \leq 1 \\ &g(t, x_1, x_2, \dots x_n) = 0 \\ &\qquad x_i(0) = \alpha_i \qquad i = 1,2,3, \dots, n \end{aligned} \tag{1}$$

Now, we give some necessary definitions of the fractional calculus theory, which are used further in this paper. There are several definitions of fractional derivative. Most important types of fractional derivatives are the Riemann-Liouville and the Caputo, which can be described as follows

Definition 2.1. A real function $f(x), x > 0$, is said to be in the space $C_\mu, \mu \in R$ if there exists a real number $p > \mu$ such that $f(x) = x^p f_1(x)$, where $f_1(x) \in C[0, \infty)$. Clearly, $C_\mu \subset C_\beta$ if $\beta < \mu$.

Definition 2.2. A function $f(x), x < 0$, is said to be in the space $C_\mu^m, m \in N \cup \{0\}$ if $f^{(m)} \in C_\mu$

Definition 2.3. The Riemann-Liouville fractional integral operator of order $\alpha \geq 0$ of a function, $f \in C_\mu,\ \mu \geq -1$, is defined as

i. $I^\alpha f(x) = \frac{1}{\Gamma(\alpha)} \int_0^x (x-t)^{\alpha-1} f(t)dt\,, \alpha > 0, x > 0$

ii. $I^0 f(x) = f(x)$

The properties of the operator I^α can be found in [16-18]. We make use of the followings.
For $f \in C_\mu,\ \mu \geq -1,\ \ \alpha, \beta \geq 0$ and $\gamma > -1$

1. $I^\alpha I^\beta f(x) = I^{\alpha+\beta} f(x)$
2. $I^\alpha I^\beta f(x) = I^\beta I^\alpha f(x)$
3. $I^\alpha x^\gamma = \frac{\Gamma(\gamma+1)}{\Gamma(\alpha+\gamma+1)} x^{\alpha+\gamma}$

Definition 2.4. The Riemann-Liouville fractional derivative of order $\alpha \geq 0$ of a function is defined as

$$D^{\alpha}f(t) = \begin{cases} \dfrac{d^{m}f(t)}{dt^{m}} & \alpha = m \in \mathbb{N} \\ \dfrac{1}{\Gamma(m-\alpha)}\dfrac{d}{dt^{m}}\displaystyle\int_0^t \dfrac{f(\tau)}{(t-\tau)^{\alpha-m+1}}dt & t > 0, 0 < m-1 < \alpha < m \end{cases}$$

III. Shannon Wavelets and Operational Matrix of the Fractional Integration

This section is devoted to introduction of Shannon wavelet bases, function approximation with these bases and establish the operational matrix of fractional integration.

i. Shannon wavelets

Wavelets are a family of functions constructed from dilation and translation of a single function called the mother wavelet. The scaling function for the Shannon multiresolution analysis is sinc function that defined on $\mathbb{R}$, and is given below

$$\varphi(t) = sinc(t) = \begin{cases} \dfrac{\sin(\pi t)}{\pi t}, & t \neq 0 \\ 1, & t = 0 \end{cases}$$

Theorem 3.1 ([19]). The function $\varphi(t)$ is a scaling function of a multiresolution analysis and the corresponding mother wavelet is defined by

$$\psi\left(t+\frac{1}{2}\right) = 2\varphi(2t) - \varphi(t)$$

Theorem 3.2 ([19]). Let j, k be non-negative integers. Then the family

$$\{\psi_{j,k}(t) = 2^{j/2}\psi(2^j t - k)\}_{j,k=0}^{\infty}$$

is an orthonormal bases of $L_2(\mathbb{R})$. j, k are dilatation and translation parameters in above theorems respectively.

ii. Reconstruction of a Function by Shannon Wavelets

In this section we express the convergence of orthogonal wavelet series when the mother wavelet is of Shannon-type. Also we show how to approximate a reasonable function with these wavelet bases.

Theorem 3.3 ([19]). Let $u(t) \in L_2(\mathbb{R}) \cap L_1(\mathbb{R})$, if $u(t)$ is of bounded variation on every bounded interval, then the wavelet series

$$u_j(t) = \sum_k \langle u, \psi_{j,k}\rangle \psi_{j,k}(t)$$

converges to $u(t)$ as $j \to \infty$ at every point of continuity of $u(t)$

Therefore, any function $u(t) \in L_2([0,1])$ have an Shannon expansion as

$$u(t) = \sum_{j=0}^{\infty}\sum_{k=0}^{\infty} c_{j,k}\psi_{j,k}(t) \tag{2}$$

where $c_{j,k} = < u(t), \psi_{j,k}(t) >$ in which $<\cdot , \cdot>$ denotes the inner product. The serie (3.1) is truncated after m-terms as

$$u(t) \cong u_m(t) = \sum_{j=0}^{m-1}\sum_{k=0}^{m-1} c_{j,k}\psi_{j,k}(t) = C^T\Psi(t) \tag{3}$$

where m denotes a positive integer, C and $\Psi(t)$ are two vectors given by

$$C = \left[c_{0,0}, c_{0,1}, \dots, c_{0,m-1}, c_{1,0}, c_{1,1}, \dots, c_{1,m-1}, \dots, c_{m-1,0}, c_{m-1,1}, \dots, c_{m-1,m-1}\right]^T$$

$$\Psi(t) = \left[\psi_{0,0}(t), \psi_{0,1}(t), \dots, \psi_{0,m-1}(t), \psi_{1,0}(t), \dots, \psi_{1,m-1}(t), \dots, \psi_{m-1,0}(t), \dots, \psi_{m-1,m-1}(t)\right]^T$$

iii. Operational matrix of the fractional integration

In this part, we may simply introduce the operational matrix of fractional integration of Shannon wavelets.

Firstly, taking the collocation points as

$$t_i = \frac{i}{m^2-1}, \quad i = mj + k,$$
$$j, k = 0, 1, \dots m-1$$

we define Shannon matrix $\Psi_{m^2 \times m^2}$ as

$$\Psi_{m^2\times m^2} = \left[\Psi(0), \Psi\left(\frac{1}{m^2-1}\right), \Psi\left(\frac{2}{m^2-1}\right) \dots, \Psi\left(\frac{m^2-2}{m^2-1}\right), \Psi(1)\right]$$

Finally, for $\boldsymbol{u}_m = [u_m(t_0), u_m(t_1) \cdots, u_m(t_{m^2-1})]^T$, the Shannon coefficients $c_{j,k}, (j, k = 0, 1, \dots m-1)$ can be obtained by

$$C^T = \boldsymbol{u}_m \Psi_{m^2\times m^2}^{-1}$$

For example, when $m = 2$ Shannon matrix is written as

$$\Psi_{4\times4} = \begin{bmatrix} 1 & 0{,}826993 & 0{,}413497 & 3{,}89817\times 10^{-17} \\ -0{,}63662 & 0{,}699057 & 0{,}699057 & -0{,}63662 \\ 0{,}212207 & 0{,}372702 & -0{,}521783 & -0{,}63662 \\ -0{,}900316 & 0{,}988616 & -0{,}737913 & 0{,}300105 \end{bmatrix}$$

Now, we need to integrate the Shannon function vector $\Psi(t)$. It can be approximated by Shannon expansion with Shannon coefficient matrix P,

$$\int_0^t \Psi(\tau)\,d\tau \approx P_{m^2\times m^2}\Psi(t)$$

where the m^2-square matrix P is called the Shannon wavelet operational matrix of integration. Our goal is to derive the Shannon wavelet operational matrix of the fractional order integration namely $P^{\alpha}_{m^2\times m^2}$. For this goal, we use m^2 −term of Block Pulse Functions on $[0,1)$ (BPFs) as follows

$$b_i(t) = \begin{cases} 1, & i\dfrac{1}{m^2} \leq t < (i+1)\dfrac{1}{m^2} \\ 0, & \text{otherwise} \end{cases}$$

where $i = 0, 1, 2, \cdots, (m^2-1)$

$b_i(t)$ functions have some useful properties like disjointness and orthogonality. Respectively that is,

$$b_i(t)\,b_l(t) = \begin{cases} 0, & i \neq l \\ b_i(t), & i = l \end{cases}$$

$$\int_0^1 b_i(\tau)\,b_l(\tau)\,d\tau = \begin{cases} 0, & i \neq l \\ 1/m^2, & i = l \end{cases}$$

Then, the Shannon wavelets can be transformed into an m^2-term block pulse functions (BPF) as

$$\Psi(t) = \Psi_{m^2\times m^2} B(t) \tag{4}$$

where

$$B(t) \triangleq [b_0(t), b_1(t), \cdots, b_{m^2-1}(t)]^T$$

Kilicman and Al Zhour [20], have introduced the Block Pulse operational matrix of the fractional order integration F^α as follows

$$(I^\alpha B)(t) \approx F^\alpha_{m^2\times m^2} B(t) \tag{5}$$

where

$$F^\alpha = \left(\frac{1}{m^2}\right)^\alpha \frac{1}{\Gamma(\alpha+2)} \begin{bmatrix} 1 & \xi_1 & \xi_2 & \cdots & \xi_{m^2-1} \\ 0 & 1 & \xi_1 & \cdots & \xi_{m^2-2} \\ 0 & 0 & 1 & \cdots & \xi_{m^2-3} \\ 0 & 0 & 0 & \ddots & \vdots \\ 0 & 0 & 0 & 0 & 1 \end{bmatrix}$$

with

$$\xi_k = (k+1)^{\alpha+1} - 2k^{\alpha+1} + (k-1)^{\alpha+1}$$

for $k = 1,2,\dots m^2-1$

Next, we derive the Shannon wavelet operational matrix of the fractional order integration.

Let

$$(I^\alpha \Psi)(t) \approx P^\alpha_{m^2\times m^2} \Psi(t) \tag{6}$$

where the m^2- square matrix $P^\alpha_{m^2\times m^2}$ is called the Shannon wavelet operational matrix of the fractional order integration.

Using Eqs. (4), (5), we get

$$(I^\alpha \Psi)(t) \approx (I^\alpha \Psi_{m^2\times m^2} B)(t) = \Psi_{m^2\times m^2}(I^\alpha B)(t) \approx \Psi_{m^2\times m^2} F^\alpha B(t) \tag{7}$$

from Eqs. (6) and (7), we get

$$P^\alpha_{m^2\times m^2}\Psi(t) = P^\alpha_{m^2\times m^2}\Psi_{m^2\times m^2}B(t) = \Psi_{m^2\times m^2}F^\alpha B(t) \tag{8}$$

Then, the Shannon wavelet operational matrix of the fractional order integration $P^\alpha_{m^2\times m^2}$ is written by

$$P^\alpha_{m^2\times m^2} = \Psi_{m^2\times m^2} F^\alpha \Psi^{-1}_{m^2\times m^2} \tag{9}$$

For example, $\alpha = 1.5$ and $m = 2$, the operational matrix $P^\alpha_{m^2\times m^2}$ is computed below

$$P^{1.5}_{4\times 4} = \begin{bmatrix} 0{,}344784 & 0{,}029417 & -0{,}648696 & 0{,}167481 \\ -0{,}017471 & -0{,}045238 & -0{,}152993 & 0{,}003118 \\ 0{,}049062 & 0{,}062126 & -0{,}048808 & -0{,}009804 \\ -0{,}125848 & 0{,}032364 & 0{,}105076 & -0{,}100288 \end{bmatrix}$$

IV. NUMERICAL EXPERIMENTS

Showing the efficiency of the method, we consider the following fractional differential-algebraic equations. All the numerical results were obtained by using the Mathematica 10.0 software

Example 4.1. We take the following fractional differential-algebraic equation.

$0 < \alpha \le 1$

$$\begin{aligned} &D^\alpha x(t) - tDy(t) + x(t) - (1+t)y(t) = 0 \\ &y(t) - sint = 0 \end{aligned} \tag{10}$$

with initial conditions $x(0) = 1,\ y(0) = 0$ and exact solutions $x(t) = e^{-t} + tsint,\ y(t) = sint$ when $\alpha = 1$
Now, we transform all terms of the equation into Shannon series form below. Firstly, let

$$Dx(t) = U^T\Psi(t) \tag{11}$$

$$Dy(t) = V^T\Psi(t) \tag{12}$$

with the initial states, we get

$$D^\alpha x(t) = U^T P^{1-\alpha}_{m^2\times m^2}\Psi(t) \tag{13}$$

$$x(t) = U^T P^1_{m^2\times m^2}\Psi(t) + \underbrace{1}_{x(0)} \tag{14}$$

$$y(t) = V^T P^1_{m^2\times m^2}\Psi(t) + \underbrace{0}_{y(0)} \tag{15}$$

Similarly, $f(t) = \sin t$ can be expanded with the Shannon coefficients below

$$f(t) = f^T_{m^2}\Psi(t) = [\sin t]_{\mathrm{ShN}} \tag{16}$$

Substituting Eqs. (11-16) into (10), we get

$$\begin{aligned} &U^T P^{1-\alpha}_{m^2\times m^2}\Psi(t) - tV^T\Psi(t) + U^T P^1_{m^2\times m^2}\Psi(t) + 1 - (1+t)V^T P^1_{m^2\times m^2}\Psi(t) = 0 \\ &V^T P^1_{m^2\times m^2}\Psi(t) - [\sin t]_{\mathrm{ShN}} = 0 \end{aligned} \tag{17}$$

Hereby, Eq. (10) has been transformed into a system of algebraic equations. Substituting values and solving the algebraic equations system, we can find the coefficients U^T. Then using Eq. (14), we can get $x(t)$. The numerical results for $m = 3,4,5$ are shown in Table 1,2,3 and Fig 1,2,3 respectively. The numerical solution is in good agreement with the exact solutions.

Table 1. Comparison of the numerical values of $x(t)$ for $m = 3$

$m=3$	α=0.25	α=0.5	α=0.75		α=1	
t	$x(t)$	$x(t)$	$x(t)$	$x(t)$	$x_{exact}(t)$	$x_{error}(t)$
t=0	0.718159	0.834216	0.907282	0.948749	1.	0.0512505
t=0.1	0.718159	0.834216	0.907282	0.948749	0.914821	0.0339287
t=0.2	0.686364	0.729621	0.802391	0.868562	0.858465	0.0100972
t=0.3	0.841455	0.805047	0.800684	0.831463	0.829474	0.00198882
t=0.4	0.920544	0.876959	0.841859	0.834009	0.826087	0.0079216
t=0.5	1.08287	0.989918	0.917579	0.872034	0.846243	0.0257907
t=0.6	1.08287	0.989918	0.917579	0.872034	0.887597	0.015563
t=0.7	1.19744	1.11038	1.01788	0.940697	0.947538	0.0068404
t=0.8	1.34758	1.24052	1.13501	1.03455	1.02321	0.0113343
t=0.9	1.46242	1.36971	1.26177	1.14762	1.11156	0.0360512

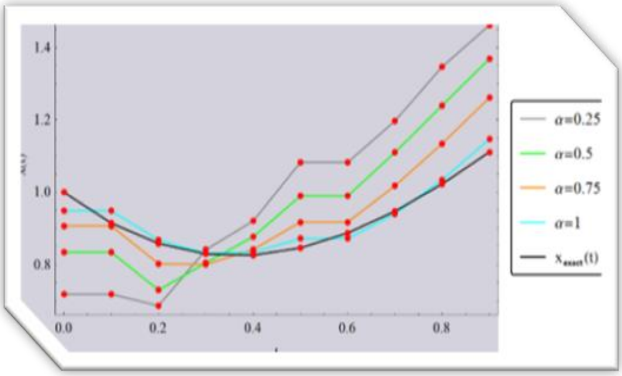

Fig 1. The graph of $x(t)$ for different values of α for $m = 3$

Table 2. Comparison of the numerical values of $x(t)$ for $m = 4$

m=4	∝=0.25	∝=0.5	∝=0.75		∝=1	
t	$x(t)$	$x(t)$	$x(t)$	$x(t)$	$x_{exact}(t)$	$x_{error}(t)$
t=0	0.755277	0.898167	0.960868	0.9851	1.	0.0149001
t=0.1	0.668525	0.758682	0.842397	0.908652	0.914821	0.00616903
t=0.2	0.734891	0.755093	0.801024	0.857432	0.858465	0.00103258
t=0.3	0.80229	0.788708	0.79753	0.830224	0.829474	0.000749809
t=0.4	0.891566	0.845801	0.821455	0.825576	0.826087	0.000511798
t=0.5	1.01993	0.946003	0.88577	0.851529	0.846243	0.00528577
t=0.6	1.12119	1.03327	0.952761	0.892594	0.887597	0.00499712
t=0.7	1.22366	1.12698	1.03187	0.949773	0.947538	0.00223485
t=0.8	1.32443	1.22407	1.1199	1.0207	1.02321	0.00251104
t=0.9	1.42115	1.3217	1.21382	1.10286	1.11156	0.00870196

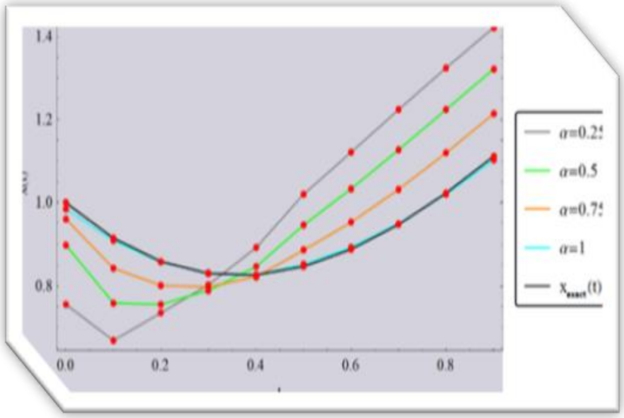

Fig 2. The graph of $x(t)$ for different values of α for $m = 4$

Table 3. Comparison of the numerical values of $x(t)$ for $m = 5$

m=5	∝=0.25	∝=0.5	∝=0.75		∝=1	
t	$x(t)$	$x(t)$	$x(t)$	$x(t)$	$x_{exact}(t)$	$x_{error}(t)$
t=0	0.808558	0.944945	0.985447	0.996139	1.	0.00386059
t=0.1	0.679012	0.76541	0.851144	0.916502	0.914821	0.00168166
t=0.2	0.727777	0.754367	0.80185	0.858814	0.858465	0.000349671
t=0.3	0.807262	0.790713	0.798005	0.829366	0.829474	0.000108214
t=0.4	0.90261	0.854189	0.826033	0.826312	0.826087	0.000224122
t=0.5	1.00732	0.935718	0.87841	0.847487	0.846243	0.00124384
t=0.6	1.10845	1.02195	0.943653	0.886413	0.887597	0.00118456
t=0.7	1.2194	1.12299	1.02838	0.94701	0.947538	0.000527254
t=0.8	1.32856	1.22814	1.12372	1.02386	1.02321	0.000649027
t=0.9	1.43283	1.33381	1.22584	1.11376	1.11156	0.00219866

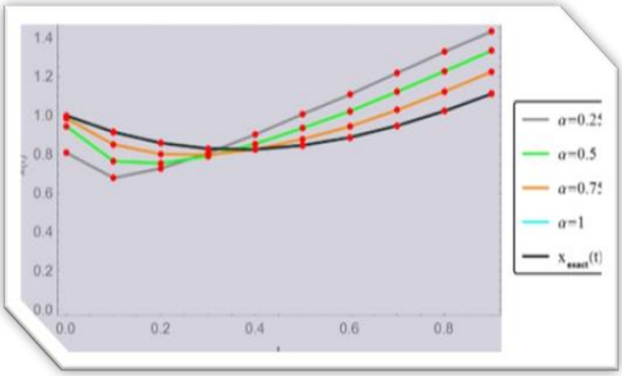

Fig 3. The graph of $x(t)$ for different values of α for $m = 5$

Example 4.2. We take the following fractional differential-algebraic equation.

$$D^{\alpha}x(t) + x(t) - y(t) = -sint$$
$$x(t) + y(t) = e^{-t} + sint \qquad (18)$$
$$0 < \alpha \le 1$$

with initial conditions $x(0) = 1,\ y(0) = 0$ and exact solutions $x(t) = e^{-t}$ and $y(t) = sint$ when $\alpha = 1$

Now, let

$$Dx(t) = R^T \Psi(t) \qquad (19)$$

$$Dy(t) = K^T \Psi(t) \qquad (20)$$

with the initial states, we have

$$D^{\alpha}x(t) = R^T P^{1-\alpha}_{m^2 \times m^2} \Psi(t) \qquad (21)$$

$$x(t) = R^T P^{1}_{m^2 \times m^2} \Psi(t) + \underbrace{1}_{x(0)} \qquad (22)$$

$$y(t) = K^T P^{1}_{m^2 \times m^2} \Psi(t) + \underbrace{0}_{y(0)} \qquad (23)$$

Similarly, the known functions in the equation

$$f(t) = sint$$
$$g(t) = e^{-t} + sint$$

can be expanded with Shannon coefficients below

$$f(t) = f^T_{m^2} \Psi(t) = [\sin t]_{ShN} \qquad (24)$$

$$g(t) = g^T_{m^2} \Psi(t) = [e^{-t} + \sin t]_{ShN} \qquad (25)$$

Substituting Eqs. (19-25) into (18), we get

$$R^T P^{1-\alpha}_{m^2 \times m^2} \Psi(t) + R^T P^{1}_{m^2 \times m^2} \Psi(t) + 1 - K^T P^{1}_{m^2 \times m^2} \Psi(t) + [\sin t]_{ShN} = 0$$

$$R^T P^{1}_{m^2 \times m^2} \Psi(t) + 1 + K^T P^{1}_{m^2 \times m^2} \Psi(t) - [e^{-t} + \sin t]_{ShN} = 0$$

(26)

Hence, Eq. (18) has been transformed into an algebraic equations system. Solving this system, we can find the coefficients R^T. Then using Eq. (22), we can get $x(t)$. The numerical results for $m = 3,4,5$ are shown in Table 4,5,6 and

Fig 4,5,6 for $x(t)$ and by same way for $y(t)$ are shown in Table 7,8,9. and Fig 7,8,9 respectively. The numerical solutions is in good agreement with the exact solutions.

Table 4. Comparison of the numerical values of $x(t)$ for $m = 3$

m = 3	∝=0.25	∝=0.5	∝=0.75		∝=1	
t	$x(t)$	$x(t)$	$x(t)$	$x(t)$	$x_{exact}(t)$	$x_{error}(t)$
t=0	0.740771	0.830452	0.89799	0.941079	1.	0.0589215
t=0.1	0.740771	0.830452	0.89799	0.941079	0.904837	0.0362411
t=0.2	0.629461	0.677678	0.753775	0.830197	0.818731	0.011466
t=0.3	0.620348	0.642125	0.673724	0.732411	0.740818	0.00840716
t=0.4	0.552602	0.578078	0.605185	0.646168	0.67032	0.0241523
t=0.5	0.541898	0.540616	0.547911	0.570099	0.606531	0.0364318
t=0.6	0.541898	0.540616	0.547911	0.570099	0.548812	0.0212872
t=0.7	0.494188	0.499459	0.498046	0.503	0.496585	0.00641461
t=0.8	0.481892	0.466772	0.454117	0.44381	0.449329	0.00551909
t=0.9	0.447091	0.435622	0.415053	0.391594	0.40657	0.0149757

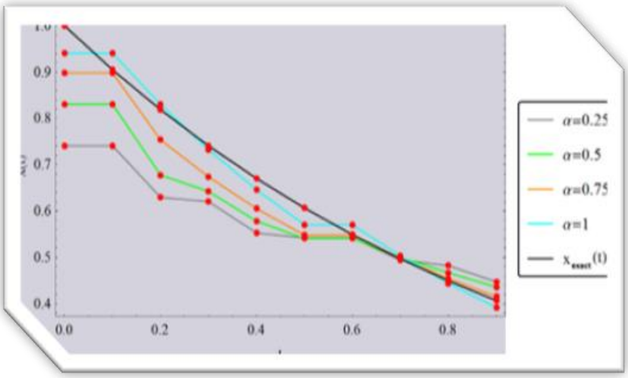

Fig 4. The graph of $x(t)$ for different values of α for $m = 3$

Table 5. Comparison of the numerical values of $y(t)$ for $m = 3$

m = 3	∝=0.25	∝=0.5	∝=0.75		∝=1	
t	$y(t)$	$y(t)$	$y(t)$	$y(t)$	$y_{exact}(t)$	$y_{error}(t)$
t=0	0.261101	0.17142	0.103883	0.060793	0.	0.0607939
t=0.1	0.261101	0.17142	0.103883	0.060793	0.099833	0.0390395
t=0.2	0.385971	0.337755	0.261658	0.185236	0.198669	0.0134337
t=0.3	0.418706	0.396929	0.36533	0.306643	0.29552	0.0111229
t=0.4	0.516723	0.491247	0.46414	0.423157	0.389418	0.0337387
t=0.5	0.561187	0.56247	0.555174	0.532987	0.479426	0.0535611
t=0.6	0.561187	0.56247	0.555174	0.532987	0.564642	0.0316558
t=0.7	0.643251	0.637979	0.639393	0.634439	0.644218	0.0097789
t=0.8	0.687864	0.702984	0.715639	0.725946	0.717356	0.0085900
t=0.9	0.750595	0.762064	0.782634	0.806093	0.783327	0.0227659

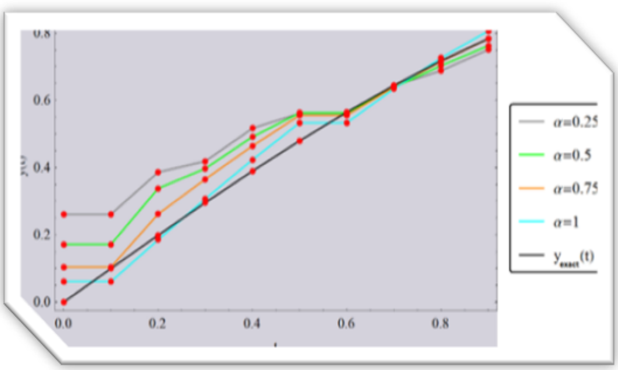

Fig 5. The graph of $y(t)$ for different values of α for $m = 3$

Table 6. Comparison of the numerical values of $x(t)$ for $m = 4$

m = 4	∝=0.25	∝=0.5	∝=0.75		∝=1	
t	$x(t)$	$x(t)$	$x(t)$	$x(t)$	$x_{exact}(t)$	$x_{error}(t)$
t=0	0.795161	0.903384	0.960563	0.984614	1.	0.0153864
t=0.1	0.676905	0.75091	0.827633	0.896485	0.904837	0.00835263
t=0.2	0.648953	0.689144	0.747001	0.816245	0.818731	0.0024854
t=0.3	0.607608	0.641041	0.683477	0.743189	0.740818	0.00237058
t=0.4	0.580252	0.600786	0.629933	0.676672	0.67032	0.0063519
t=0.5	0.544298	0.554566	0.568868	0.597151	0.606531	0.00937943
t=0.6	0.520223	0.523946	0.528777	0.543706	0.548812	0.00510517
t=0.7	0.498754	0.496064	0.492542	0.495045	0.496585	0.00153984
t=0.8	0.478835	0.47051	0.459554	0.45074	0.449329	0.001411
t=0.9	0.460617	0.446988	0.429373	0.4104	0.40657	0.00383038

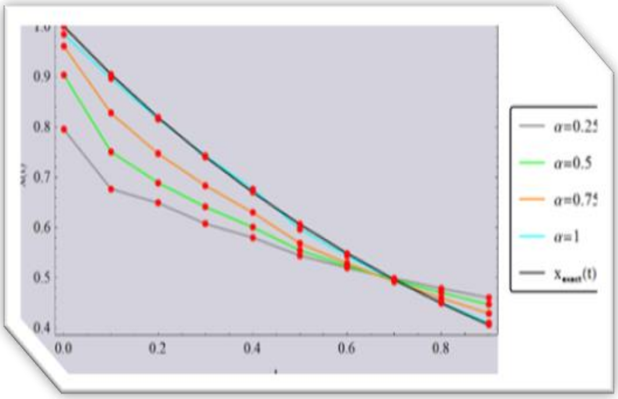

Fig 6. The graph of $x(t)$ for different values of α for $m = 4$

*Table 7.*Comparison of the numerical values of $y(t)$ for $m = 4$

m = 4	∝=0.25	∝=0.5	∝=0.75		∝=1	
t	$y(t)$	$y(t)$	$y(t)$	$y(t)$	$y_{exact}(t)$	$y_{error}(t)$
t=0	0.20496	0.0967363	0.039558	0.0155072	0.	0.0155072
t=0.1	0.328647	0.254642	0.177918	0.109066	0.0998334	0.0092330
t=0.2	0.368954	0.328763	0.270906	0.201662	0.198669	0.0029925
t=0.3	0.428062	0.39463	0.352194	0.292481	0.29552	0.0030387
t=0.4	0.477148	0.456614	0.427467	0.380728	0.389418	0.0086900
t=0.5	0.545908	0.53564	0.521338	0.493055	0.479426	0.0136292
t=0.6	0.595822	0.5921	0.587269	0.572339	0.564642	0.0076967
t=0.7	0.642886	0.645576	0.649099	0.646595	0.644218	0.0023774
t=0.8	0.687076	0.695401	0.706357	0.715171	0.717356	0.0021853
t=0.9	0.727248	0.740876	0.758491	0.777464	0.783327	0.0058628

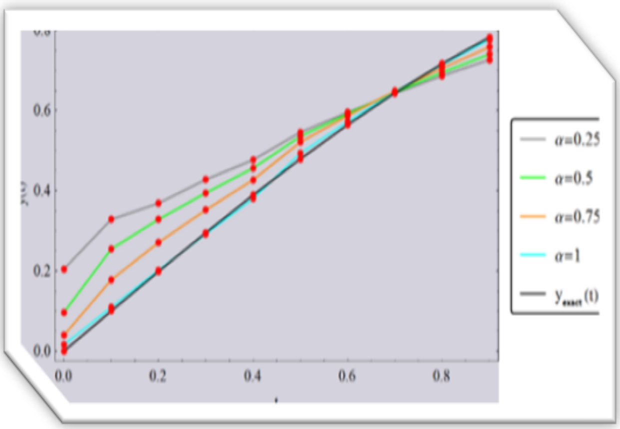

Fig 7. The graph of $y(t)$ for different values of α for $m = 4$

Table 8. Comparison of the numerical values of $x(t)$ for $m = 5$

m = 5	∝=0.25	∝=0.5	∝=0.75		∝=1	
t	$x(t)$	$x(t)$	$x(t)$	$x(t)$	$x_{exact}(t)$	$x_{error}(t)$
t=0	0.837625	0.947223	0.985487	0.996108	1.	0.003891
t=0.1	0.694830	0.762959	0.839847	0.906966	0.904837	0.002129
t=0.2	0.645960	0.691372	0.750024	0.819375	0.818731	0.000644
t=0.3	0.608269	0.639287	0.681130	0.740242	0.740818	0.000575
t=0.4	0.575881	0.596161	0.623803	0.668753	0.67032	0.001566
t=0.5	0.547148	0.558630	0.574218	0.604167	0.606531	0.002363
t=0.6	0.523189	0.527625	0.533584	0.550100	0.548812	0.001288
t=0.7	0.499571	0.497186	0.494000	0.496974	0.496585	0.000388
t=0.8	0.478068	0.469498	0.458257	0.448978	0.449329	0.000350
t=0.9	0.458432	0.444184	0.425791	0.405617	0.40657	0.000951

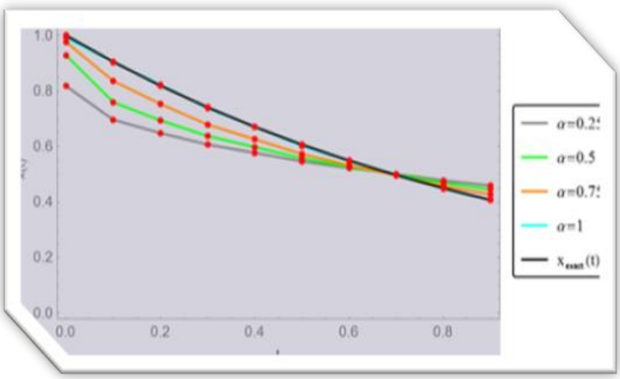

Fig 8. The graph of $x(t)$ for different values of α for $m = 5$

Table 9. Comparison of the numerical values of $y(t)$ for $m = 5$

m = 5	∝=0.25	∝=0.5	∝=0.75		∝=1	
t	$y(t)$	$y(t)$	$y(t)$	$y(t)$	$y_{exact}(t)$	$y_{error}(t)$
t=0	0.162382	0.052784	0.01452	0.0038986	0.	0.00389869
t=0.1	0.309632	0.241502	0.164614	0.0974953	0.099833	0.00233816
t=0.2	0.371313	0.325902	0.26725	0.197899	0.198669	0.00077010
t=0.3	0.428237	0.397219	0.355376	0.296263	0.29552	0.00074306
t=0.4	0.484445	0.464165	0.436523	0.391574	0.389418	0.00215538
t=0.5	0.539867	0.528386	0.512797	0.482848	0.479426	0.00342282
t=0.6	0.589617	0.58518	0.579222	0.562705	0.564642	0.00193698
t=0.7	0.641022	0.643407	0.646593	0.643619	0.644218	0.00059834
t=0.8	0.68881	0.69738	0.708621	0.7179	0.717356	0.00054380
t=0.9	0.731967	0.746215	0.764608	0.784782	0.783327	0.00145472

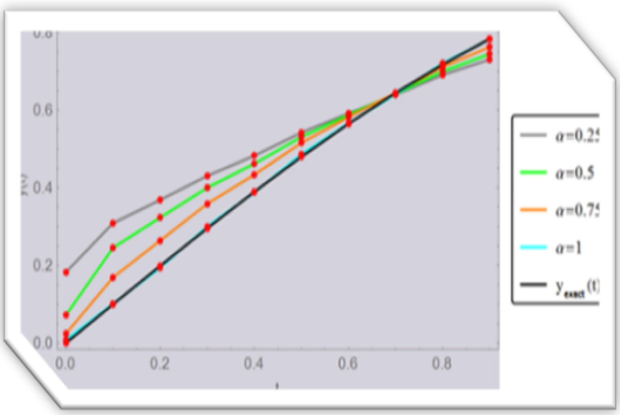

Fig 9. The graph of $y(t)$ for different values of α for $m = 5$

V. CONCLUSION

In this paper, the Shannon wavelet functions has been employed to solve fractional differential-algebraic equations (FDAEs). The results obtained by the method are in good agreement with the given exact solutions. The study show that the method is effective techniques to solve fractional differential–algebraic equations, and the method presents real advantages in terms of comprehensible applicability and precision

REFERENCES

[1] F. Mainardi, Fractional calculus: Some basic problems in continuum and statistical mechanics, in: A. Carpinteri, F. Mainardi (Eds.), Fractals and Fractional Calculus in Continuum Mechanics, Springer, New York, 1997, pp.291-348.

[2] R. Hilfer, Applications of Fractional Calculus in Physics. World Scientific, Singapore, 2000.

[3] A.B. Malinowska, D.F.M. Torres, Towards a combined fractional mechanics and quantization. Fractional Calculus and Applied Analysis 15, No 3 (2012), 407–417

[4] A. Carpinteri, F Mainardi. Fractals and Fractional Calculus in Continuum Mechanics, Springer Verlag, Wien, NewYork, 1997

[5] T. Kaczorek, Positive linear systems consisting of n subsystems with different fractional orders. IEEE Transactions on Circuits and Systems I 58(2011), 1203–121

[6] B. İbiş. M. Bayram . Numerical comparison of methods for solving fractional differential-algebraic equations (FDAEs), Computers and Mathematics with Applications 62 (2011) 3270-3278

[7] B. Ibiş, M. Bayram, A. Göksel Agargun, Applications of fractional differential transform method to fractional differential-algebraic equations. European Journal of Pure and Applied Mathematics 4(2011), 129–141.

[8] M. Karabacak, E. Çelik. The numerical solution of fractional differential-algebraic equations (FDAEs), New Trends in Mathematical Sciences, Vol.1 No.1 (2013), pp 106.

[9] M. Yiğider, E. Çelik . The numerical solution of partial differential-algebraic equations, Advances in Difference Equations (2013) 2013:8

[10] E. Khodadadi ,M. Karabacak, Solving fuzzy fractional partial differential equations by fuzzy Laplace-Fourier transforms. Journal of Computational Analysis and Applications, Vol. 19, No.2, pp.260-271, Eudoxus Press LLC, 2015

[11] V. Turut ,E. Çelik, M. Yiğider. Multivariate padé approximation for solving partial differential equations (PDE), International Journal for Numerical Methods in Fluids, vol 66, (2011) 1159-1173.

[12] K. Nouri, NB. Siavashani, Application of Shannon wavelet for solving boundary value problems of fractional differential equations, Wavelets and Linear Algebra 1 (2014) 33-42

[13] C. Cattani, "Shannon wavelets theory," Mathematical Problems in Engineering, vol. 2008, Article ID 164808, 24 pages, 2008.

[14] C. Cattani, "Connection coefficients of Shannon wavelets," Mathematical Modelling and Analysis, vol. 11, no. 2, pp. 117–132, 2006.

[15] M. Zurigat, S. Momani, A. Alawneh. Analytical approximate solutions of systems of fractional algebraic–differential equations by homotopy analysis method, Comput. Math. Appl. 59 (3) (2010) 1227–1235.

[16] I. Podlubny. Fractional Differential Equations. An Introduction to Fractional Derivatives Fractional Differential Equations Some Methods of their Solution and Some of their Applications, Academic Press, San Diego, 1999.

[17] KS Miller, B. Ross. An Introduction to the Fractional Calculus and Fractional Differential Equations, John Wiley and Sons Inc., New York, 1993.

[18] K. Oldham, J. Spanier, The Fractional Calculus, Academic Press, New York, 1974.

[19] JJ. Benedetto, PJSG. Ferreira, Modern Sampling Theory, Springer Science and Business Media, New York, 2001.

[20] A. Kilicman, ZAA. Al Zhour, Kronecker operational matrices for fractional calculus and some applications, Appl. Math. Comput. 187 (2007) 250–265